



AN h - p FINITE ELEMENT VIBRATION ANALYSIS OF OPEN CONICAL SANDWICH PANELS AND CONICAL SANDWICH FRUSTA

N. S. BARDELL, R. S. LANGLEY,[†] J. M. DUNSDON AND G. S. AGLIETTI

*Department of Aeronautics and Astronautics, University of Southampton,
Highfield, Southampton SO17 1BJ, England*

(Received 21 September 1998, and in final form 9 April 1999)

The vibration study of a general three-layer conical sandwich panel based on the h - p version of the finite element method is presented in this paper. No restriction is placed on the degree of curvature of the shell, thereby relaxing the strictures associated with shallow shell theory. The methodology incorporates a new set of trigonometric functions to provide the element p -enrichment, and elements may be joined together to model either open conical panels, or complete conical frusta (circumferentially connected, but open at each end). The full range of classical boundary conditions, which includes free, clamped, simply supported and shear diaphragm edges, may be applied in any combination to open and closed panels, thereby facilitating the study of a wide range of conical sandwich shells. The convergence properties of this element have been established for different combinations of the h - and p -parameters, thereby assuring its integrity for more general use. Since very little work has been reported on the vibration characteristic of either circumferentially closed or open conical sandwich panels, the main thrust of this work has been to present and validate an efficient modelling technique, rather than to perform numerous parameter and/or sensitivity studies. To this end, some new results are presented and subsequently validated using a commercially available finite element package. It is shown that for results of comparable accuracy, models constructed using the h - p formulation require significantly fewer degrees of freedom than those assembled using the commercial package. Some preliminary experimental results are also included for completeness.

© 1999 Academic Press

1. INTRODUCTION

1.1. BACKGROUND

The motivation for the present work has arisen from a renewed interest in the use of sandwich construction as the primary structural medium in the vicinity of the engine exhaust outlets for commercial aircraft with turbojet, turboprop or propfan engines mounted at the rear of the fuselage [1]. The structural topology of

[†] Now at The Department of Engineering, Trumpington Street, University of Cambridge, CB2 1PZ, U.K.

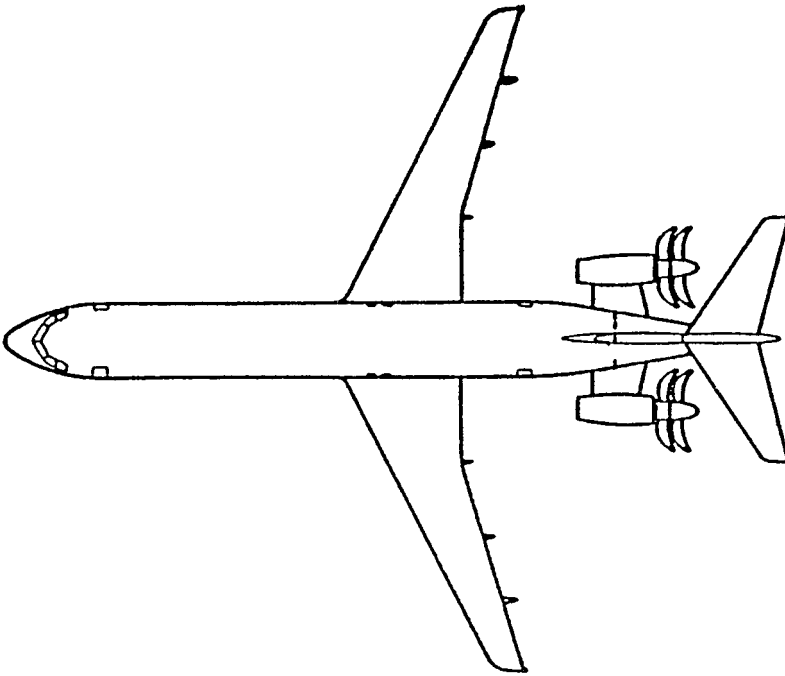


Figure 1. A typical proposed installation arrangement for a propfan-powered civil aircraft, illustrating how the rear fuselage is tapered in a near-conical fashion.

the fuselage in the region of the exhaust ducts/propeller plane is more likely to form part of a conical surface than a cylindrical one (due to the tapering of the tail section—see Figure 1), although it is not readily apparent what effect a non-uniform radius of panel curvature might have on the vibration response. The most likely form of construction would follow the standard practice of attaching a number of (open) sandwich panels to an internal substructure of ribs and stringers, to provide a stiff, light-weight, built-up, monocoque shell structure. These considerations provide the initial justification for a vibration study of a single, open, conical sandwich panel.

In service, such panels will be subjected not only to static loads, like internal pressurization and inertia forces, but also to a variety of intense, randomly fluctuating pressure and temperature loads which will induce severe vibration levels in an elevated thermal environment. Under such conditions, due allowance must be made for the static pre-stresses, the likelihood of large deflection amplitudes, and the structural damage-accumulation arising from acoustic and thermal fatigue. Although such a detailed non-linear analysis, including the effect of thermal degradation of the faceplate and core material properties, is the ultimate goal of this research, it is important that this capability is realized from a proven history of successive incremental work programmes, each of which has been thoroughly validated before proceeding to the next stage. Hence, the study presented here is best regarded as a preliminary investigation, deliberately limited to a linear, temperature-independent, free-vibration analysis of all-metallic open conical sandwich panels having isotropic face-plates and generally orthotropic honeycomb

cores.[†] As a precursor to more advanced studies, not only will this work provide a useful datum against which the validity of future research work can be assessed, but moreover it will make a significant contribution to the literature in its own right, since it would appear to be the first paper specifically to address the topic of free vibration of an open conical sandwich panel. The most likely reason for such a surprising lacuna can be attributed directly to the analytical difficulties involved; for a circumferentially closed, right circular cone or frustum, the two-dimensional nature of the assumed displacement field can be reduced to a quasi one-dimensional axisymmetric problem through Fourier decomposition of the circumferential wavemotion—for an *open* conical sandwich panel, no such simplification exists, and resort must be made to a full two-dimensional solution scheme. Such a scheme will inevitably be complicated further by the dependence of the circumferential arc length on its meridional location.

1.2. LITERATURE REVIEW

The general subject area of sandwich construction has been well researched over the past 50 years, with many significant contributions dedicated to the dynamic behaviour of sandwich beams, plates, and, to a lesser extent, cylinders. However, very little has been reported on the vibration of *conical* sandwich panels, despite their obvious connection with, and extensive use in, a variety of aerospace applications. Indeed, every article found to date has been devoted entirely to the vibration analysis of circumferentially closed sandwich frusta and cones; although this literature is not of immediate relevance to the title problem, it nonetheless provides an appropriate reference point which will help position the current work.

Azar [2] is credited with being one of the first investigators to address the axisymmetric free vibration problem of an arbitrary sandwich shell of revolution, although he made no direct reference to conical panels. The earliest work devoted specifically to conical sandwich frusta was reported in a series of seminal papers [3–5] by Bert and his co-investigators during the late 1960s and early 1970s. Bert *et al.* recognized the value of adopting a Rayleigh–Ritz energy approach, and took advantage of the fact that the functions assumed for the displacements and core rotations in the circumferential sense could conveniently be decomposed into their constituent Fourier components. The functions assumed for the displacements and core rotations in the lengthwise direction were chosen to satisfy the geometric boundary conditions at either end of the conical frustum that were of particular interest—hence the [slight] difference between references [4, 5]. It is certain that much of the initial motivation for the work on conical sandwich shells was provided by the all-consuming quest of the United States during the 1960s to “*land a man on the moon and return him safely to the earth*”. It is therefore not surprising that apart from a single publication by Gupta and Jain [6] in 1978, no subsequent developments were reported until the early 1990s, by which time large-scale

[†]In the near to medium term future, metallic materials will continue to be used as primary structure in the close proximity of engine exhaust outlets.

computing technology had matured (thereby rendering the complex analysis task considerably more tractable than had hitherto been the case), and when different applications for conical sandwich shells were being explored [7–9].

The increasing use of layered composites resulted in further research activity during the mid-1990s. Ramesh and Ganesan [10–12] developed an energy-based model using an assumed linear piecewise approximation for the in-plane displacement of each layer through the thickness, and an assumed circumferential displacement variation using Fourier expansions. Their latter work [12] concentrated on the vibration and damping characteristics of a three-layered conical shell with a viscoelastic core constrained by isotropic facing materials; the semi-analytical finite element method they developed was based upon the displacement field originally proposed by Wilkins, Bert and Egle [5], and the results they presented were also based on the panel dimensions and properties first quoted in reference [5]. Khatri [13–15], and Khatri and Asnani [16, 17] used a variational approach to derive the differential equations governing the motion of a layered conical shell, and proceeded to find approximate solutions for the natural frequencies and modes using Galerkin's method. Since each layer was shear deformable, a few studies were presented of a conical sandwich panel which could be regarded as a special case of a three-layered shell, with shear-stiff outer layers to represent isotropic/orthotropic face plates. However, the work reported in reference [16] (and presumably reference [17]) has rightly been criticized by Baruch [18] on the grounds that the elastic constants for each layer are actually a function of their spatial position, and not independent constants as assumed by Khatri and Asnani.

Finally, two important and comprehensive literature surveys which provide significant background material that is relevant to the issues described herein are worth mentioning. Noor *et al.* [19] have charted in great detail the design and analysis of sandwich structures ranging from simple beams to doubly curved shells; a complementary overview of shallow shell theory has been given by Liew *et al.* [20]. Together, these surveys provide a fitting conclusion to the literature review presented herein.

1.3. MODELLING CONSIDERATIONS

Mathematical models of sandwich-type structural forms must take account of the shear deformable nature of the core material, which, in a displacement-type of formulation, is usually accounted for by the use of additional degrees of freedom (d.o.f) to represent the shear deformation [21]. It is well-known that approximately four conventional finite elements are required to capture one half-wavelength of vibration in a given direction [22]. Upon considering that most “sandwich shell elements” are actually constructed from three separate layers, each with four nodes and six d.o.f. per node, it soon becomes apparent that the total number of d.o.f. in a two-dimensional model capable of capturing, say, the first 10 modes of vibration, is extremely large, and will most likely prove prohibitively expensive for recursive analyses such as optimization or sensitivity studies. It is against this background that the h - p version of the FEM [23–27] is presented, since this formulation promises substantial efficiency gains without loss of accuracy when compared with

the conventional FEM. The novelty of the solution scheme developed in this paper is further enhanced by the use of the highly versatile set of trigonometric p -functions first proposed by Beslin and Nicolas [28].

Whilst certain aspects of the h - p methodology described in this paper (i.e., its use as a single super-element) might appear to bear a superficial resemblance to other global Ritz-type procedures (such as the pb -2 technique advocated by Lim and Liew [29]), it is sufficiently distinct to justify its appellation as a genuine FEM. Since the h - p version of the FEM reported here is formulated on an individual conical element basis, it possesses at least three characteristics which distinguish it from the global technique described in reference [29].

- (i) Shells with cut-outs and/or irregular boundaries could be modelled. (This feature is not readily apparent here since only a right conical panel is being considered.)
- (ii) The general nature of the formulation means that the structural stiffness and mass matrices are completely generic and have only to be computed once—specific boundary conditions can then be applied in any combination and in any order. This is significantly more versatile than the pb -2 approach reported in reference [29], in which the assumed displacement field is boundary condition dependent and therefore has to be constructed specifically for each particular boundary problem. In this context, it should be noted that the h - p approach presented here permits an open conical sandwich panel or a closed conical sandwich frustum to be modelled with equal facility and robustness—this level of versatility is simply not possible with the pb -2 approach, which would require quite different definitions of the circumferential displacement field in order to model each case.
- (iii) The h - p method can be tailored to the problem in hand to provide an efficient solution. For example, consider the vibration of a circumferentially closed shell, in which a relatively large number of half waves can establish themselves around the circumference in a given mode. A global Ritz approach would have to include a large number of terms in its description of the assumed displacement field to capture these modes with confidence—this is computationally expensive. In contrast, the h - p method reported here enables the finite element mesh to be subdivided around the circumference, thereby providing a much more natural and efficient modelling technique for this sort of problem.

1.4. SCOPE OF THE WORK

It should by now be evident that the amount of work pertaining to the free vibration of completely closed conical sandwich shells is actually quite meagre, and, as stated earlier, the case of an open conical sandwich panel remains wholly unsolved. The purpose of this paper can therefore best be summarized as follows:

- (i) To produce an efficient and reliable analytical model capable of providing solutions for the natural frequencies and associated normal modes of generic conical sandwich panels, using the h - p version of the FEM;

- (ii) To validate this formulation against known results for (a) open conical sandwich panels and (b) complete conical sandwich frusta; since there is no other published work fulfilling remit (a), verification will have to be made against results forthcoming from a proprietary finite element package; remit (b) can partially be fulfilled by making reference to existing work in the open literature, but some additional finite element results will also be included for completeness.
- (iii) To provide some initial experimental results for some specific open conical sandwich panels, and to use these results as the basis for a comparison with the theoretical analysis, given the absence of other numerical data; to this end, four different conical sandwich panels—each fabricated with aluminium face plates and overexpanded aluminium cores [30]—were produced for testing.

2. METHOD

2.1. ASSUMPTIONS

As with all work of this kind, a set of initial assumptions [21] must be made with the aim of capturing the essential properties of the physical conical sandwich panel, whilst permitting an analytically tractable solution to be obtained. For the problem under consideration, this set may be summarized as follows.

- (i) There is no significant direct strain in the core perpendicular to the plane of the face plates. Hence, both the face plates and the core deflect by the same amount normal to the plate surface.
- (ii) There is no significant shear strain across the depth of the face plates. Hence, only the core will carry the shear strain, which is assumed *uniform* through the core depth.
- (iii) The face plates are considered to be isotropic, and to possess both axial and flexural stiffness.
- (iv) The core is considered to be generally orthotropic, and to possess both axial and flexural stiffness.
- (v) The sandwich plate is assumed to behave elastically, and is subject to small displacements.

In what follows, the lower face-plate will be referred to as layer 1, the core as layer 2, and the upper face-plate as layer 3. The mid-plane of layer 2 is taken as the global reference datum from which all subsequent deformations are measured. (Note that this reference datum will not coincide with the geometric mid-plane of a panel whose face-plates are not of equal thickness.)

2.2. ASSUMED DEFORMATION PATTERN

Consider a particle at a general point x, θ, z_2 within layer 2. In its deformed state, the position of this particle is related to the layer 2 mid-plane displacements by

$$u_2(x, \theta, z_2) = u_{02} + z_2\psi, \quad v_2(x, \theta, z_2) = v_{02} + z_2\chi; \quad w_2(x, \theta, z_2) = w_{02}, \quad (1a-c)$$

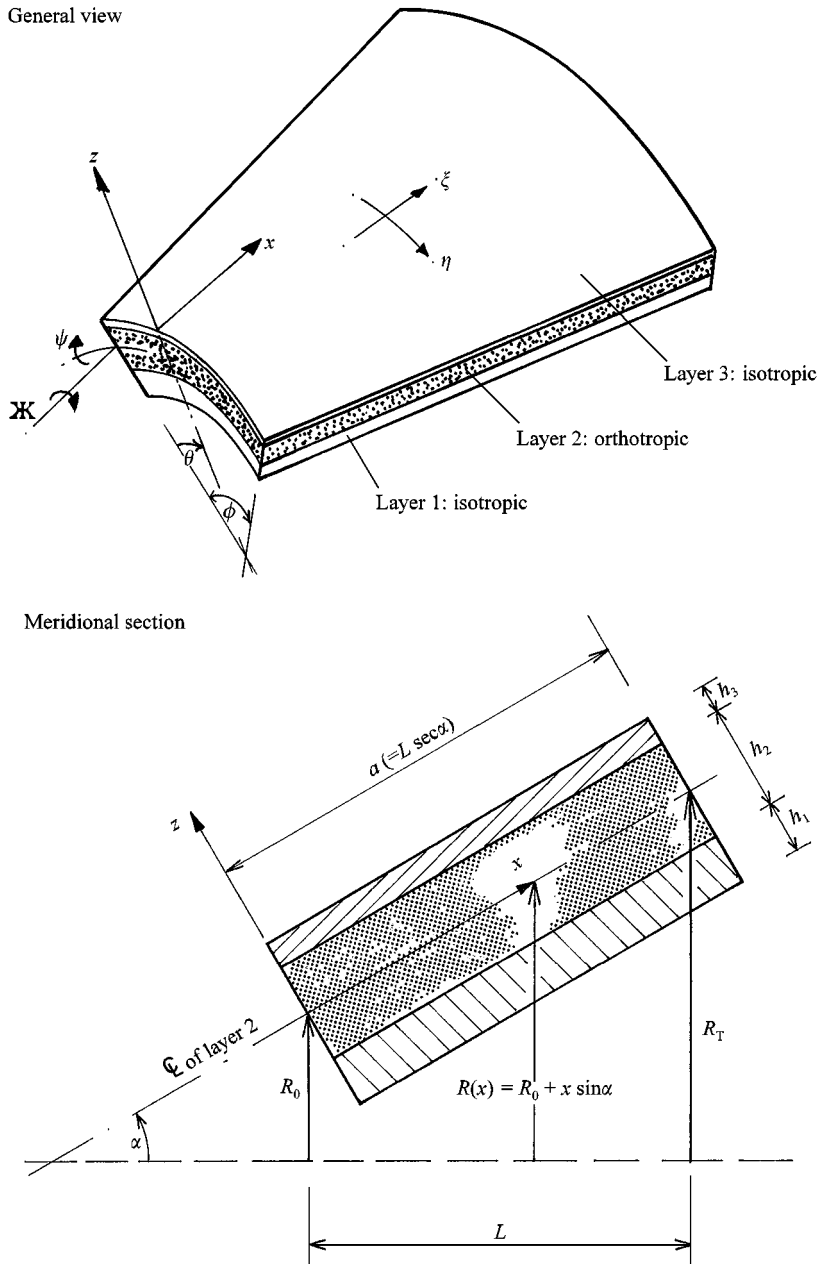


Figure 2. The conical sandwich panel element. The core ribbon direction is parallel to the cone generator.

where u_{02} , v_{02} , and w_{02} are the displacements of the layer 2 mid-plane, and \mathcal{K}^\ddagger and ψ are the rotations due to shear deformation of layer 2 about the x - and θ -axis respectively; see Figure 2. Equations (1) can be rendered in matrix

[‡]In effect, $\mathcal{K} = [v_{02} \cos \alpha - (\partial w_{02} / \partial \theta)] / R(x)$, on account of the v_2 displacement taking place along the curved θ co-ordinate direction.

format as

$$\begin{bmatrix} u_2 \\ v_2 \\ w_2 \end{bmatrix} = \begin{bmatrix} 1 & 0 & 0 & z_2 & 0 \\ 0 & 1 & 0 & 0 & z_2 \\ 0 & 0 & 1 & 0 & 0 \end{bmatrix} \begin{bmatrix} u_{02} \\ v_{02} \\ w_{02} \\ \psi \\ \mathcal{K} \end{bmatrix} \tag{1d}$$

i.e.,

$$\delta_2 = \mathbf{R}_2 \delta_{02}, \tag{1e}$$

where δ_{02} is the vector of layer 2 mid-plane displacements. By similar reasoning, the displacement of a particle at a general point (x, θ, z_3) within layer 3 is related to the layer 3 mid-plane by

$$u_3(x, \theta, z_3) = u_{03} - z_3 \partial w_{03} / \partial x, \tag{2a}$$

$$v_3(x, \theta, z_3) = v_{03} + z_3 [-(\partial w_{03} / \partial \theta) / R(x) + v_{03} \cos \alpha / R(x)], \tag{2b}$$

$$w_3(x, \theta, z_3) = w_{03} = w_{02}, \tag{2c}$$

where u_{03}, v_{03} and w_{03} are the displacements of the layer 3 mid-plane; see Figure 3. Compatibility between layers 2 and 3 is enforced by ensuring that every particle on the upper surface of layer 2 occupies the same position as every particle on the lower surface of layer 3, i.e., There is no relative slippage permitted between the core and face-plate. Hence, by equating equations (1a), (1b) and (1c) with z_2 set equal to $h_2/2$, to equations (2a), (2b), and (2c) with z_3 set equal to $-h_3/2$ respectively, the following compatibility relationship is established:

$$\begin{bmatrix} u_{03} \\ v_{03} \\ w_{03} \end{bmatrix} = \begin{bmatrix} 1 & 0 & -\frac{h_3}{2} \frac{\partial}{\partial x} & \frac{h_2}{2} & 0 \\ 0 & \frac{1}{\left(1 - \frac{h_3}{2} \frac{\cos \alpha}{R(x)}\right)} & -\frac{h_3}{2 R(x)} \frac{\partial}{\partial \theta} & 0 & \frac{h_2}{\left(1 - \frac{h_3}{2} \frac{\cos \alpha}{R(x)}\right)} \\ 0 & 0 & 1 & 0 & 0 \end{bmatrix} \begin{bmatrix} u_{02} \\ v_{02} \\ w_{02} \\ \psi \\ \mathcal{K} \end{bmatrix}. \tag{3a}$$

Equations (3a) can be written more compactly as

$$\delta_{03} = \mathbf{R}_3 \delta_{02}. \tag{3b}$$

In a similar manner, enforcing compatibility between layers 2 and 1 yields

$$\begin{bmatrix} u_{01} \\ v_{01} \\ w_{01} \end{bmatrix} = \begin{bmatrix} 1 & 0 & -\frac{h_1}{2} \frac{\partial}{\partial x} & -\frac{h_2}{2} & 0 \\ 0 & \frac{1}{\left(1 + \frac{h_1}{2} \frac{\cos \alpha}{R(x)}\right)} & \frac{\frac{h_1}{2} \frac{\partial}{\partial \theta}}{\left(1 + \frac{h_1}{2} \frac{\cos \alpha}{R(x)}\right)} & 0 & \frac{-h_2}{\left(1 + \frac{h_1}{2} \frac{\cos \alpha}{R(x)}\right)} \\ 0 & 0 & 1 & 0 & 0 \end{bmatrix} \begin{bmatrix} u_{02} \\ v_{02} \\ w_{02} \\ \psi \\ \mathcal{K} \end{bmatrix} \quad (4a)$$

Equation (4a) can be written more compactly as

$$\delta_{01} = \mathbf{R}_1 \delta_{02} \quad (4b)$$

2.3. STRAIN-DISPLACEMENT RELATIONSHIP

The strain–displacement relationships [31] for the conical outer face skins (layers 1 and 3), related to their own mid-planes, are

$$\begin{bmatrix} \varepsilon_{xx} \\ \varepsilon_{\theta\theta} \\ \gamma_{x\theta} \end{bmatrix}_{1,3} = \begin{bmatrix} \frac{\partial}{\partial x} & 0 & -z_{1,3} \frac{\partial^2}{\partial x^2} \\ \frac{\sin \alpha}{R(x)} & \frac{1}{R(x)} \left(1 + z_{1,3} \frac{\cos \alpha}{R(x)}\right) \frac{\partial}{\partial \theta} & \frac{\cos \alpha}{R(x)} - z_{1,3} \frac{1}{R(x)^2} \frac{\partial^2}{\partial \theta^2} - z_{1,3} \frac{\sin \alpha}{R(x)} \frac{\partial}{\partial x} \\ \frac{1}{R(x)} \frac{\partial}{\partial \theta} \frac{\partial}{\partial x} - \frac{\sin \alpha}{R(x)} - z_{1,3} \frac{2 \cos \alpha \sin \alpha}{R(x)^2} + z_{1,3} \frac{2 \cos \alpha}{R(x)} \frac{\partial}{\partial x} & -z_{1,3} \frac{2}{R(x)} \frac{\partial^2}{\partial x \partial \theta} + z_{1,3} \frac{2 \sin \alpha}{R(x)^2} \frac{\partial}{\partial \theta} \end{bmatrix} \begin{bmatrix} u_{01,03} \\ v_{01,03} \\ w_{01,03} \end{bmatrix} \quad (5)$$

where subscripts 1 and 3 refer to the appropriate face-plate. The two equations shows in expression (5) may be written in the form

$$\varepsilon_1 = \mathbf{F}_1 \delta_{01} \quad \text{and} \quad \varepsilon_3 = \mathbf{F}_3 \delta_{03} \quad (6a, b)$$

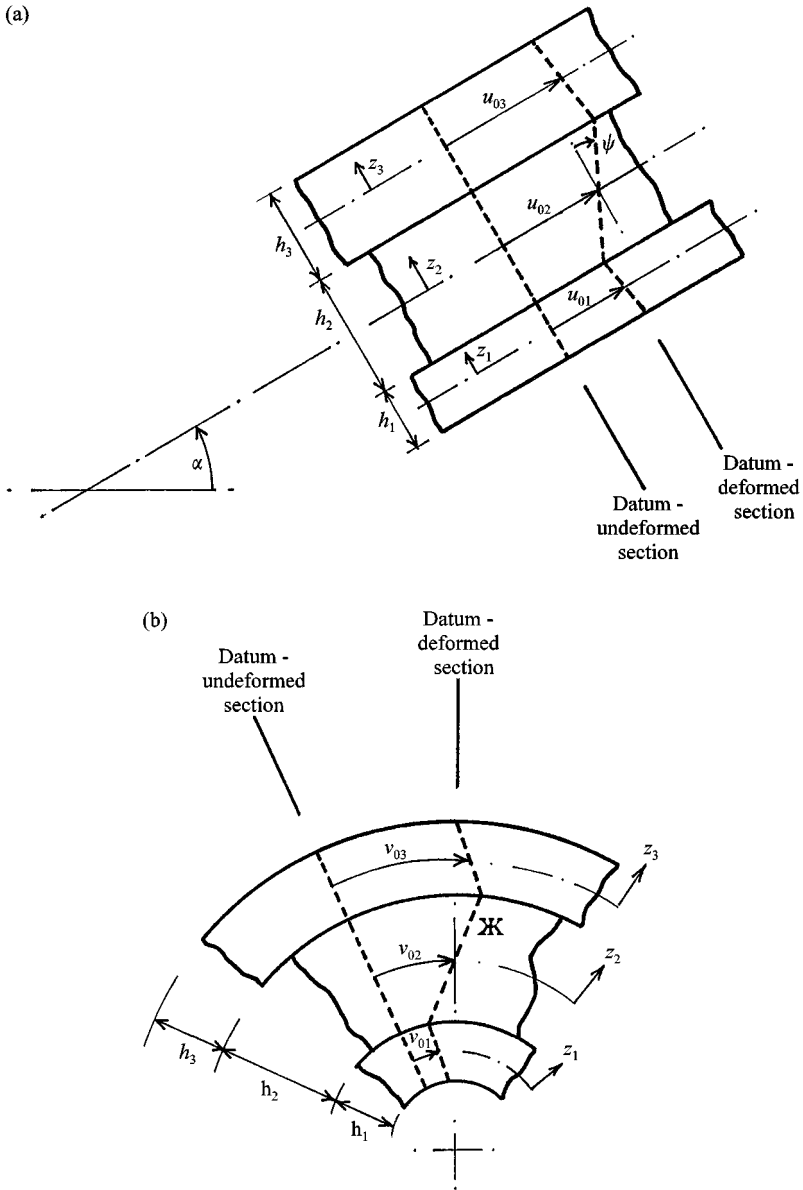


Figure 3. The assumed deformation patterns (shown in the x and θ directions). (a) Meridional assumed displacement pattern within each layer; (b) Circumferential displacement pattern within each layer.

In order to relate these face-plate displacements to the core mid-plane displacements, it is necessary to use equations (3b) and (4b) such that $\varepsilon_1 = \mathbf{F}_1 \mathbf{R}_1 \delta_{02}$ and

$$\varepsilon_3 = \mathbf{F}_3 \mathbf{R}_3 \delta_{02}, \text{ i.e.,}$$

$$\varepsilon_1 = A_1 \delta_{02} \quad \text{and} \quad \varepsilon_3 = \Lambda_3 \delta_{02}, \tag{6c, d}$$

where $A_1 = \mathbf{F}_1 \mathbf{R}_1$ and $A_3 = \mathbf{F}_3 \mathbf{R}_3$. The strain–displacement relationship for the shear deformable core can be written [31] as

$$\begin{bmatrix} \varepsilon_{xx} \\ \varepsilon_{\theta\theta} \\ \gamma_{\theta z} \\ \gamma_{xz} \\ \gamma_{x\theta} \end{bmatrix}_2 = \begin{bmatrix} \frac{\partial}{\partial x} & 0 & 0 & z_2 \frac{\partial}{\partial x} & 0 \\ \frac{\sin \alpha}{R(x)} & \frac{1}{R(x)} \frac{\partial}{\partial \theta} & \frac{\cos \alpha}{R(x)} & z_2 \frac{\sin \alpha}{R(x)} & z_2 \frac{1}{R(x)} \frac{\partial}{\partial \theta} \\ 0 & -\frac{\cos \alpha}{R(x)} & \frac{1}{R(x)} \frac{\partial}{\partial \theta} & 0 & 1 \\ 0 & 0 & \frac{\partial}{\partial x} & 1 & 0 \\ \frac{1}{R(x)} \frac{\partial}{\partial \theta} & \frac{\partial}{\partial x} - \frac{\sin \alpha}{R(x)} + z_2 \frac{\cos \alpha}{R(x)} \frac{\partial}{\partial x} & 0 & z_2 \frac{1}{R(x)} \frac{\partial}{\partial \theta} & z_2 \left(\frac{\partial}{\partial x} - \frac{\sin \alpha}{R(x)} \right) \end{bmatrix} \begin{bmatrix} u_{02} \\ v_{02} \\ w_{02} \\ \psi \\ \mathcal{K} \end{bmatrix} \tag{7a}$$

$$\varepsilon_2 = A_2 \delta_{02} . \tag{7b}$$

Note. The entry in the second column of the fifth row of the above, A_2 matrix consists of three terms. Soedel [31] only mentions the first two of these in his work; the third term, which is dependent on z_2 , must be present in order that equation (7a) reduces to equation (5) for a conical panel in which the shear deformation effects are negligible. Hence the authors have included it in this work.

It is convenient at this stage to render equations (1)–(7) in terms of non-dimensional element-local co-ordinates ξ, η which are related to the element Cartesian co-ordinates through $\xi = (2x/a) - 1$ and $\eta = (2\theta/\phi) - 1$, where ϕ is the total angle subtended by the mid-plane circumference of the panel; see Figure 2. Note also that every occurrence of $R(x)$ is replaced by $b(x)/\phi$, which in turn can be written as $b(\xi)/\phi$, since $b(x) \equiv b(\xi)$, so that there is only one ξ -dependent term ($b(\xi)$) in any given expression.

2.4. LAYER CONSTITUTIVE RELATIONS

The standard constitutive relations [31] for the isotropic face plates, and the generally orthotropic core, are written as follows:

$$\begin{bmatrix} \sigma_{xx} \\ \sigma_{\theta\theta} \\ \tau_{x\theta} \end{bmatrix}_{1,3} = \begin{bmatrix} \frac{E}{(1-\nu^2)} & \frac{\nu E}{(1-\nu^2)} & 0 \\ \frac{\nu E}{(1-\nu^2)} & \frac{E}{(1-\nu^2)} & 0 \\ 0 & 0 & G \end{bmatrix}_{1,3} \begin{bmatrix} \varepsilon_{xx} \\ \varepsilon_{\theta\theta} \\ \gamma_{x\theta} \end{bmatrix}_{1,3} ,$$

$$\begin{bmatrix} \sigma_{xx} \\ \sigma_{\theta\theta} \\ \tau_{\theta z} \\ \tau_{zx} \\ \tau_{x\theta} \end{bmatrix}_2 = \begin{bmatrix} \frac{E_x}{(1 - \nu_{x\theta} \nu_{\theta x})} & \frac{\nu_{\theta x} E_x}{(1 - \nu_{x\theta} \nu_{\theta x})} & 0 & 0 & 0 \\ \frac{\nu_{x\theta} E_\theta}{(1 - \nu_{x\theta} \nu_{\theta x})} & \frac{E_\theta}{(1 - \nu_{x\theta} \nu_{\theta x})} & 0 & 0 & 0 \\ 0 & 0 & G_{\theta z} & 0 & 0 \\ 0 & 0 & 0 & G_{zx} & 0 \\ 0 & 0 & 0 & 0 & G_{x\theta} \end{bmatrix}_2 \begin{bmatrix} \varepsilon_{xx} \\ \varepsilon_{\theta\theta} \\ \gamma_{\theta z} \\ \gamma_{zx} \\ \gamma_{x\theta} \end{bmatrix},$$

$$\sigma_{1,3} = \mathbf{D}_{1,3} \varepsilon_{1,3} \quad \text{and} \quad \sigma_2 = \mathbf{D}_2 \varepsilon_2. \tag{8a, b}$$

2.5. CHOICE OF ASSUMED DISPLACEMENT FUNCTIONS; BACKGROUND TO THE *h-p* VERSION OF THE FEM

The *h-p* methodology adopted is similar to that presented elsewhere by the authors [32], so only the essential details are given here. In brief, the *h-p* version of the FEM may be regarded as the marriage of the conventional *h*-version and *p*-version; convergence is sought by simultaneously refining the mesh and increasing the degree of the elements [23–27]. For the type of problem under consideration here, in which the motion in all five d.o.f.s is coupled, it is advantageous to represent all the displacement fields by the *same* set of assumed modes. This greatly reduces the computational effort required to calculate the element stiffness and mass matrices, and simplifies the element assembly process.

To this end, an ascending hierarchy of special trigonometric functions [28], used in conjunction with Hermite cubics, will furnish a complete set of admissible displacement functions $f(\xi \text{ or } \eta)$; see Table 1. The motivation for using trigonometric, as opposed to the usual *K*-orthogonal polynomial [32] hierarchical functions, is on account of their improved performance when modelling medium frequency deformations.

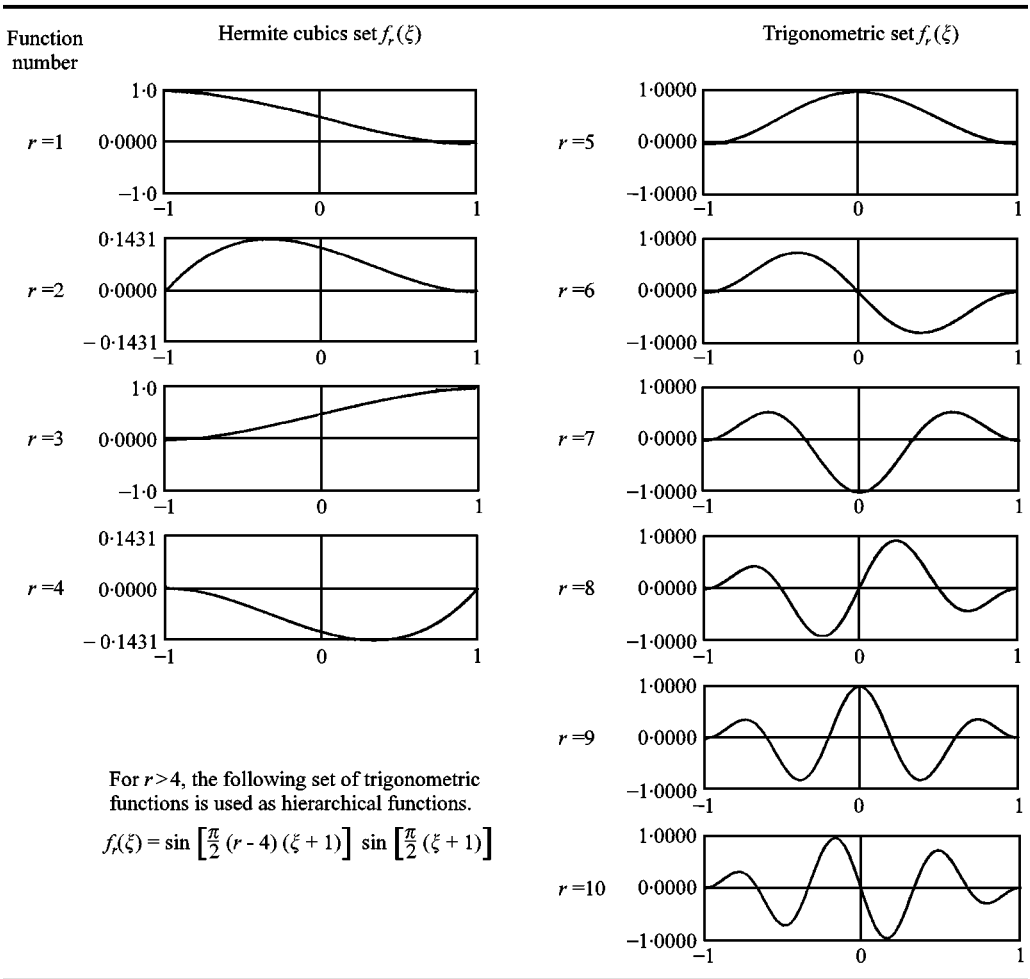
The hierarchical modes contribute only to the internal displacement field of the element, and do not therefore affect the displacement along the element edge or at the element nodes. However, products formed between any of the trigonometric functions and the Hermite cubics will constitute what amounts to edge freedoms along the element boundaries. Adjacent elements may be joined by ensuring compatibility of both nodal and edge displacements. The use of what effectively amounts to C_1 continuity functions to describe the in-plane and shear deformation displacement fields—which possess C_0 continuity—is justified on the grounds that no attempt is made to enforce *first derivative continuity* of any of these quantities across an element interface.

Hence the in-plane, out-of-plane and shear deformation master displacements can be represented as the following series expressions:

$$u_0(\xi, \eta) = \sum_{r=1}^{P_{ux}} \sum_{s=1}^{P_{uy}} X_{r,s} f_r(\xi) f_s(\eta), \quad v_0(\xi, \eta) = \sum_{r=1}^{P_{vx}} \sum_{s=1}^{P_{vy}} Y_{r,s} f_r(\xi) f_s(\eta) \tag{9a, b}$$

TABLE 1

The first 10 assumed displacement functions



$$w_0(\xi, \eta) = \sum_{r=1}^{p_{wx}} \sum_{s=1}^{p_{wy}} Z_{r,s} f_r(\xi) f_s(\eta), \quad \psi(\xi, \eta) = \sum_{r=1}^{p_{yx}} \sum_{s=1}^{p_{yy}} \Psi_{r,s} f_r(\xi) f_s(\eta) \tag{9c, d}$$

$$\mathcal{H}(\xi, \eta) = \sum_{r=1}^{p_{\mathcal{H}x}} \sum_{s=1}^{p_{\mathcal{H}y}} \mathcal{H}_{r,s} f_r(\xi) f_s(\eta). \tag{9e}$$

This can be expressed in a more compact matrix notation as

$$\delta_0 = \mathbf{N} \mathbf{q}, \tag{9f}$$

where $\mathbf{q}^T = [X_{r,s}, Y_{r,s}, Z_{r,s}, \Psi_{r,s}, \mathcal{H}_{r,s}]$ and \mathbf{N} is a rectangular matrix with 5 rows.

2.6. PANEL ENERGIES

The strain energy of the panel, which is given by

$$U = \frac{1}{2} \sum_{i=1}^3 \int_{V_i} \boldsymbol{\varepsilon}_i^T \mathbf{D}_i \boldsymbol{\varepsilon}_i dV_i. \quad (10)$$

can be constructed from equations (1–9) as

$$U = \frac{1}{2} \mathbf{q}^T \left[\frac{a}{4} \sum_{i=1}^3 \int_{-1}^1 \int_{-1}^1 \int_{-h_i/2}^{+h_i/2} (\mathbf{A}_i \mathbf{N})^T \mathbf{D}_i (\mathbf{A}_i \mathbf{N}) b(\xi) dz_i d\xi d\eta \right] \mathbf{q}. \quad (11)$$

The terms within parentheses are recognized as the element stiffness matrix \mathbf{K}^E .

Similarly, the kinetic energy of the panel element is given by

$$T = \frac{1}{2} \sum_{i=1}^3 \int_{V_i} \rho_i \dot{\boldsymbol{\delta}}_i^T \dot{\boldsymbol{\delta}}_i dV_i \quad (12)$$

Substituting equations (1e), (3b), (4b) and (9) into equation (12) yields

$$T = \frac{1}{2} \dot{\mathbf{q}}^T \left[\frac{a}{4} \sum_{i=1}^3 \int_{-1}^1 \int_{-1}^1 \int_{-h_i/2}^{+h_i/2} \rho_i (\mathbf{R}_i \mathbf{N})^T (\mathbf{R}_i \mathbf{N}) b(\xi) dz_i d\xi d\eta \right] \dot{\mathbf{q}}. \quad (13)$$

The terms within parentheses are recognized as the element mass matrix \mathbf{M}^E . Note that in-plane inertia and rotary deformation effects are contained within this expression on account of the coupling that exists between the various displacements characterizing each layer. It is also worth pointing out that \mathbf{A}_i and \mathbf{R}_i both contain differential operators, rendering the evaluation of the stiffness and mass matrices shown, respectively, in equations (11) and (13) far from trivial. Symbolic computing was used to determine the form of these integrands, but the subsequent matrix multiplication and integration required to evaluate them was performed numerically by using a Gauss–Legendre quadrature scheme. This scheme, which was implemented by using commercially available software [33], dynamically allocates the number of integration points required to ensure a pre-determined level of accuracy.

Inter-element compatibility is achieved simply by matching the appropriate generalized co-ordinates at common element nodes and along common edges, as explained earlier. This procedure ensures the elements are fully conforming—in the conventional sense—and, moreover, facilitates assembly of the global stiffness and mass matrices \mathbf{K}^G and \mathbf{M}^G .

Note: To join elements in an x -wise sense, the radius of curvature and semi-vertex angle must be the same at the (curved) element interface.

2.7. BOUNDARY CONDITIONS

Specific boundary conditions may be applied to the model simply by removing those rows/columns from \mathbf{K}^G and \mathbf{M}^G which correspond to fixed d.o.f.—hence any combination of shear diaphragm, simple support, clamped or free edges, or corner point supports, can be accommodated in the analysis. In the current work, the support conditions are imposed at the layer 2 mid-plane, so some care has to be

taken in defining exactly what each category means. A shear diaphragm permits an in-plane translation across, and full rotations about, the mid-plane but prevents w -wise motion normal to it; a simple support permits full rotation of the panel about its mid-plane, but prevents all three translational freedoms there; a clamped support prevents all three translational freedoms and shear deformation within layer 2.

2.8. EQUATIONS OF MOTION

By assuming simple harmonic motion, and the absence of any forcing agency, the governing equations of motion for free vibration can be obtained by deriving Lagrange's equation from the expressions already obtained for the strain and kinetic energies of the complete model. This yields the standard matrix-eigenvalue form of the problem:

$$[\mathbf{K}^G - \omega^2 \mathbf{M}^G] \{\mathbf{q}\} = 0. \quad (14)$$

The solution of equation (14) gives the natural frequencies in radian units, rendered here in an appropriate form depending on the analysis. Corresponding to each eigenvalue is an eigenvector which may be used in conjunction with equation (9) to recover the associated displacement of each element in the model, and hence the complete mode of the panel under consideration.

3. COMPARISON WITH OTHER WORK

3.1. CONVERGENCE STUDY FOR OPEN CONICAL SANDWICH PANELS

In order to gain confidence with the h - p formulation presented here, it is important to validate the convergence behaviour of the model. As mentioned in section 1, the absence of any published results for open conical panels means that any work presented here will likely serve as a benchmark for future analyses of this type. To this end, convergence results are presented for a typical open conical sandwich panel (whose defining properties are given in Table 2), with additional verification provided by a comprehensive finite element analysis using the commercially available package ANSYS [34].

Six different trade-off studies were conducted for this panel using various combinations of the h - and p -parameters. These results are also presented in Table 2. It is immediately obvious that the results from the current method converge monotonically and from above, as expected, and that very good agreement is obtained with the results forthcoming from ANSYS.

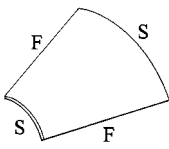
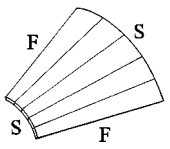
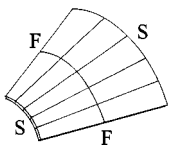
The relatively slow convergence of the low-frequency results stems from the use of the trigonometric assumed displacement functions; this feature has been noted by their progenitors [28]. Whilst the single-element, with the highest possible amount of p -enrichment, will clearly give the most accurate results for the least overall number of d.o.f., it nonetheless can be computationally advantageous to consider more creative mesh designs—such as the $h = 5$, $p = 9$ combination illustrated in Table 2—since the low-frequency modes of the panel are likely to

TABLE 2

(a) *Material and geometric properties defining the typical open conical sandwich panel used to assess the convergence behaviour of the h-p methodology*

Open sandwich cone no. 1 (symmetric section)							
Material properties	Thickness (mm)	Elastic modulus (GPa)	Poisson's ratio	Shear modulus (GPa)			Density (kg/m ³)
Layer 1 (aluminium)	1.0	70.0	0.30				2700
Layer 2 (aluminium honeycomb core)	8.0	0.0	N/A	$G_{x\theta} = 0$	$G_{zx} = 0.15$	$G_{\theta z} = 0.05$	120.0
Layer 3 (aluminium)	1.0	70.0	0.30				2700
Geometry relative to the mid-plane of layer 2:	Panel boundary conditions along the edges given by:		ϕ (deg)	L (mm)	α (deg)	R_o (mm)	R_T (mm)
	$x = 0$	$x = a$	$\theta = 0$	$\theta = \phi$			
	S	S	F	F			

(b) *Convergence properties of the current h-p method for an open sandwich panel (natural frequencies in Hz)*

Current h-p version $h = 1$	Current h-p version $h = 5$	Current h-p version $h = 10$	FEM [†] 720 elements (13 176 d.o.f.)
			
$p = 8$ 272 d.o.f.	$p = 6$ 544 d.o.f.	$p = 5$ 619 d.o.f.	
$f_1 = 170.2$ $f_2 = 175.4$ $f_3 = 332.9$ $f_4 = 350.3$ $f_5 = 363.2$ $f_6 = 384.0$	$f_1 = 166.3$ $f_2 = 172.6$ $f_3 = 331.9$ $f_4 = 342.3$ $f_5 = 358.1$ $f_6 = 381.5$	$f_1 = 164.7$ $f_2 = 171.1$ $f_3 = 330.6$ $f_4 = 340.3$ $f_5 = 356.6$ $f_6 = 380.7$	163.4 169.8 328.4 336.8 353.1 376.2
$p = 10$ 440 d.o.f.	$p = 9$ 1471 d.o.f.	$p = 8$ 2128 d.o.f.	same as above
$f_1 = 166.6$ $f_2 = 172.5$ $f_3 = 331.3$ $f_4 = 343.9$ $f_5 = 358.7$ $f_6 = 381.4$	$f_1 = 164.2$ $f_2 = 170.6$ $f_3 = 330.2$ $f_4 = 339.4$ $f_5 = 355.8$ $f_6 = 380.3$	$f_1 = 163.7$ $f_2 = 170.1$ $f_3 = 329.7$ $f_4 = 338.4$ $f_5 = 354.9$ $f_6 = 379.9$	

[†]The face plates and core were modelled by using Shell 91, a dedicated sandwich shell element having eight nodes per element with six d.o.f. per node.

involve significantly more deformation around the panel's circumference than along its length. Whichever mesh is used, the h - p methodology still provides very accurate results from models with significantly fewer d.o.f. than those used in conventional finite element analyses.

The first six modes of this open sandwich panel are shown in Figure 4, illustrating low-frequency bending modes with the typical deformation pattern mentioned above. Notice how the amplitude of a given mode decreases towards the panel "apex" on account of the reducing panel radius causing an increase in the local bending stiffness.

Since the low-frequency modes of this panel involve a reasonable amount of deformation around the circumference, a sufficient number of assumed shape functions and/or h -element divisions needs to be included in the analysis to capture this motion. This sort of behaviour has been well documented for cylinders and other singly curved structures, so its occurrence here comes as no surprise.

3.2. CONVERGENCE STUDY FOR CIRCUMFERENTIALLY JOINED CONICAL SANDWICH FRUSTA

Ramesh and Ganesan [10] presented various frequency and mode results for conical sandwich frusta based on the earlier work of Sui and Bert [4] and Wilkins *et al.* [5]. Since these cases have been well documented, it seems reasonable to use them as the basis for a limited convergence study. The panel details are given in Table 3(a), and two different sets of circumferential boundary conditions were used in keeping with reference [10], namely both ends clamped and both ends supported on shear-diaphragms.[†]

The circumferentially continuous nature of a conical frustum suggests that at low frequencies it will likely vibrate with considerably more half-waves around its circumference than along its length. This observation leads to a rather different modelling strategy from the usual one adopted for an open panel—it will now be more advantageous to divide the circumference of the frustum into considerably more elements than the length. In this manner, a modest p -boost can be used in each element such that the anticipated circumferential and lengthwise motions are adequately represented by the assumed displacement pattern provided by the model. (Obviously, a single element could also have been used, but this was not considered computationally efficient on account of the high degree of polynomial enrichment that would have been necessary.)

To illustrate the above reasoning, two different convergence studies are presented for each cone; the results are shown in Tables 3(b, c). The results from the current h - p method are seen to converge monotonically and from above to yield frequencies marginally lower than those cited by Ramesh and Ganesan [10] and Wilkins *et al.* [5]. It should be noted from Tables 3(b, c) that the methods used by both previous groups of investigations [5, 10] have failed to capture some of the

[†]Ramesh and Ganesan referred to their end condition as a simple support, which they defined as one which suppressed circumferential and radial displacements. Since they did not suppress the longitudinal displacement over the support, then strictly speaking the terminology "shear diaphragm" should have been used—this parlance has been adopted in the present work.

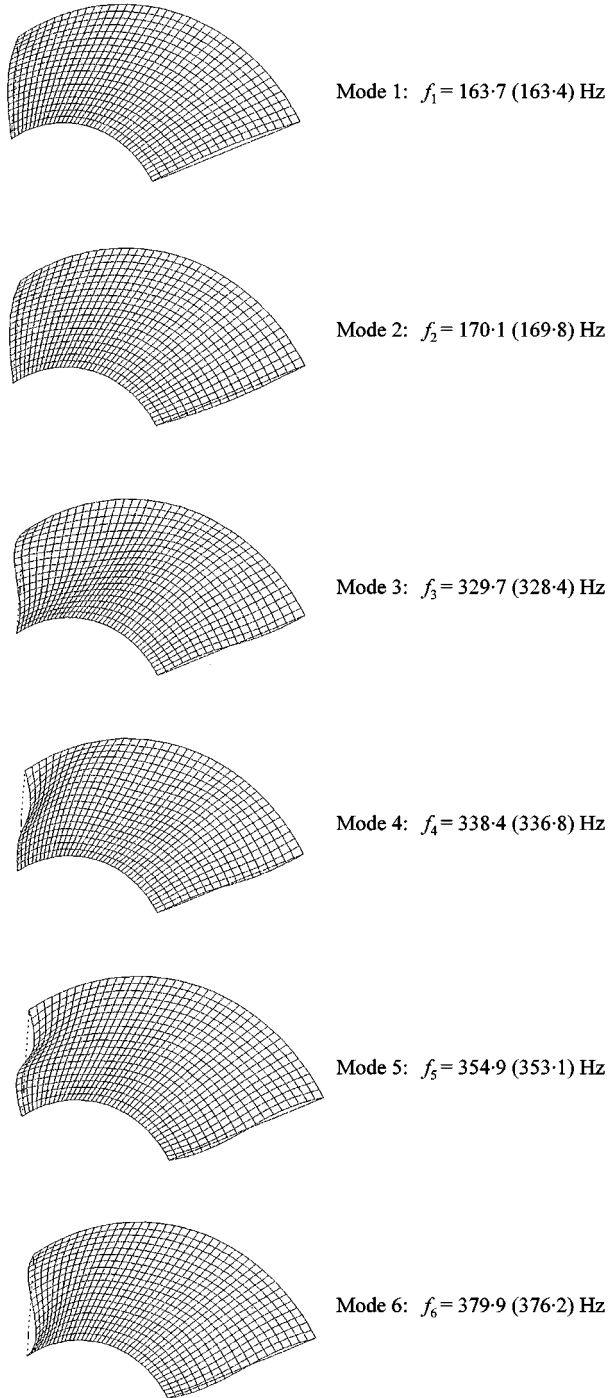


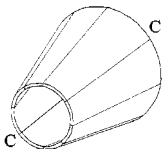
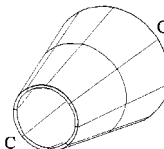
Figure 4. The first six natural frequencies and modes of a typical open conical sandwich panel with its circumferential ends simply supported. (h - p results quoted with $h = 10$ and $p = 8$; ANSYS results in parentheses).

TABLE 3

(a) *Material and geometric properties defining the complete conical sandwich frustum used to assess the convergence behaviour of the h-p methodology*

Complete sandwich frustum (after Ramesh and Ganesan [10])							
Material properties	Thickness (mm)	Elastic modulus (GPa)	Poisson's ratio	Shear modulus (GPa)			Density (kg/m ³)
Layer 1 (glass epoxy)	0.535	25.59	0.20	7.03			2800
Layer 2 (aluminium honeycomb)	7.62	0.0	N/A	$G_{x\theta} = 0.0$	$G_{zx} = 0.2249$	$G_{\theta z} = 0.1286$	36.8
Layer 3 (glass epoxy)	0.535	25.59	0.20	7.03			2800
Geometry relative to the mid-plane of layer 2:	ϕ (deg)	L (mm)	α (deg)	R_o (mm)	R_r (mm)		
	360	1834.3	5.07	570.2	732.9		

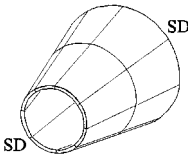
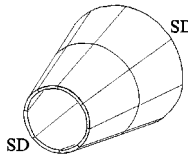
(b) *Convergence properties of the current h-p method for the frustum described in Table 3(a); the ends $x = 0$ and $x = a$ are clamped around their circumference. (Natural frequencies in Hz)*

Natural frequencies in ascending order	Current h-p version $h = 8$	Current h-p version $h = 16$	FEM [†] [34] Fully converged results using a total of 912 elements with 15 840 d.o.f.	Ramesh and Ganesan [10]	Wilkins <i>et al.</i> [5]
					
f_1	120.2	108.3 (4, 1)	107.3 (4, 1)	110.9 (4, 0)	110.7 (4, 1)
f_2	136.1	122.3 (3, 1)	119.7 (3, 1)	128.5 (3, 0)	126.0 (3, 1)
f_3	136.2	125.8 (5, 1)	126.8 (5, 1)	126.3 (5, 0)	126.7 (5, 1)
f_4	174.1	163.5 (6, 1)	165.8 (6, 1)	—	—
f_5	$p = 6$ 189.5	$p = 8$ 173.5 (2, 1)	170.9 (2, 1)	185.6 (2, 0)	177.2 (2, 1)
f_6	480 226.6	2736 186.2 (5, 2)	182.9 (5, 2)	188.6 (5, 1)	197.7 (5, 2)
f_7	d.o.f. 290.7	d.o.f. 195.7 (4, 2)	190.0 (4, 2)	202.3 (4, 1)	209.1 (4, 2)
f_8	291.3	206.8 (6, 2)	206.6 (6, 2)	—	—
f_9	335.6	212.4 (7, 1)	215.2 (7, 1)	—	—
f_{10}	340.8	240.5 (3, 2)	234.7 (3, 2)	252.9 (3, 1)	252.9 (3, 2)

[†]The face plates and core were modelled by using Shell 91, a dedicated sandwich shell element having eight nodes per element with six d.o.f. per node.

TABLE 3. Continued

(c) Convergence properties of the current h - p method for the frustum described in Table 3(a); the ends $x = 0$ and $x = a$ are supported on shear-diaphragms (SD) around their circumference. (Natural frequencies in Hz)

Natural frequencies in ascending order	Current h - p version $h = 8$	Current h - p version $h = 16$	FEM [†] [34] Fully converged results using a total of 912 elements with 16 608 d.o.f.	Ramesh and Ganesan [10]	Wilkins <i>et al.</i> [5]
					
f_1	84.4	84.1 (3, 1)	85.5 (3, 1)	85.5 (4, 0)	85.7 (4, 1)
f_2	84.7	84.6 (4, 1)	85.6 (4, 1)	89.4 (3, 0)	86.8 (3, 1)
f_3	114.3	113.6 (5, 1)	115.7 (5, 1)	113.3 (5, 0)	113.3 (5, 1)
f_4	134.7	134.6 (2, 1)	136.3 (2, 1)	145.1 (2, 0)	134.8 (2, 1)
f_5	$p = 6$ 157.2	$p = 6$ 155.8 (6, 1)	158.6 (6, 1)	—	—
f_6	880 164.4	1584 163.2 (5, 2)	166.5 (5, 2)	167.7 (5, 1)	160.6 (5, 2)
f_7	d.o.f. 168.6	d.o.f. 167.8 (4, 2)	170.9 (4, 2)	177.6 (4, 1)	165.4 (4, 2)
f_8	194.4	192.2 (6, 2)	196.1 (6, 2)	—	—
f_9	208.0	205.4 (7, 1)	208.8 (7, 1)	—	—
f_{10}	216.5	216.0 (3, 2)	219.8 (3, 2)	222.1 (3, 1)	212.8 (3, 2)

[†]The face plates and core were modelled by using Shell 91, a dedicated sandwich shell element having eight nodes per element with six d.o.f. per node.

low-frequency modes (i.e., of the first 10 modes which occur below 240 Hz, the 4th, 8th, and 9th are missing), and thus their results form an incomplete set. The veracity of the current results is confirmed further by an independent, fully converged, finite element analysis, the results of which are also presented in Tables 3(b, c). From the level of agreement demonstrated here, it can be concluded that the h - p formulation works very efficiently for circumferentially closed conical sandwich frusta.

Since the frequency results forthcoming from the current h - p method provide no immediate indication of the number of complete waves around the circumference (m) and the number of half-waves along the length (n), it was necessary to determine this information indirectly by plotting the corresponding natural modes. As an example, the first 10 modes for the (well-converged) clamped case are presented in Figure 5 from which the (m, n) classifications are clearly visible. It should be noted here that Ramesh and Ganesan used an usual nomenclature to describe the number of half-waves along the length of the shell (actually $n - 1$), which explains the variance when compared with the present work and that of Bert *et al.*

One final observation of interest has been made concerning the second case considered here, in which the shell is supported around its circumference by shear

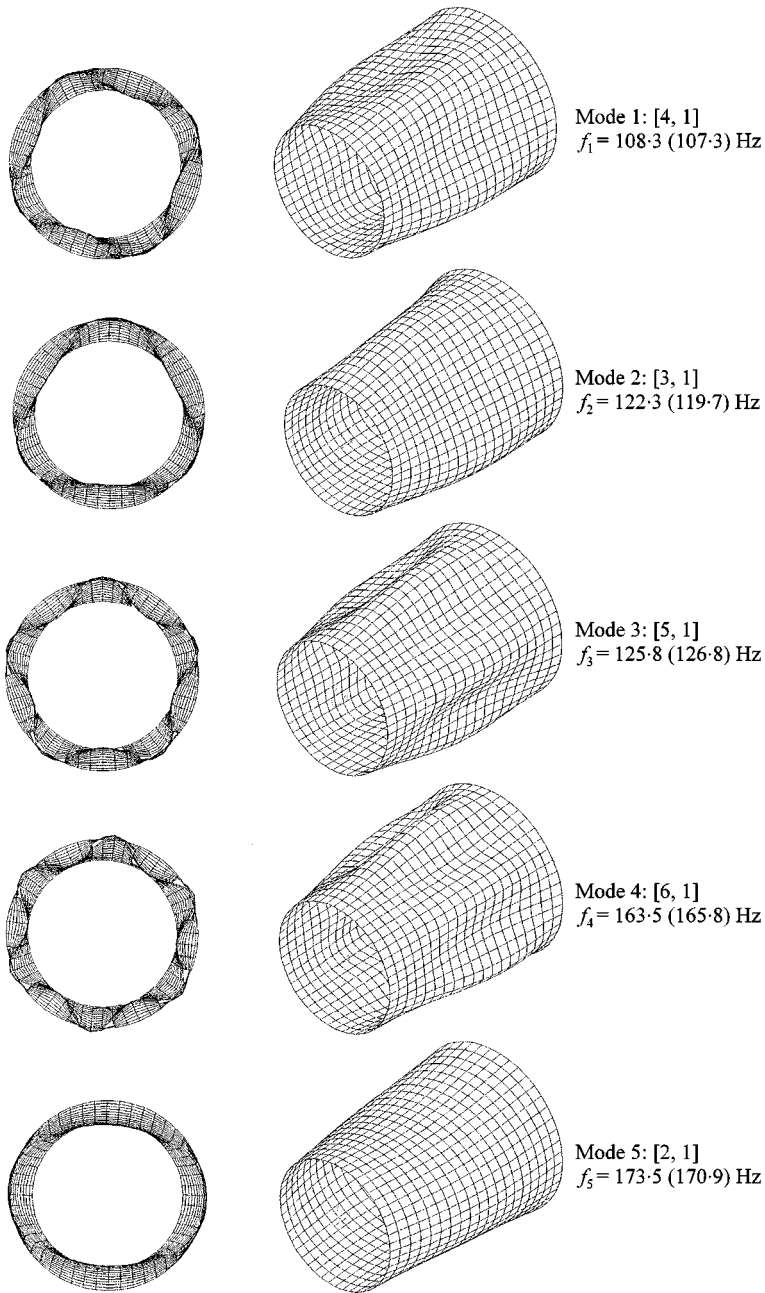


Figure 5. Identification of the (m, n) classification using the modal information for a circumferentially clamped conical sandwich frustum. The panel details are described in Table 3(a), and the natural frequencies are given in Table 3(b).

diaphragms. The lowest frequency of vibration actually occurs at 13.1 Hz^\dagger although this result has not been included in Table 3(c). This frequency corresponds to a longitudinal back and forth motion of the conical shell passing over its

[†]The ANSYS model also captured this mode, which occurred at 13.0 Hz .

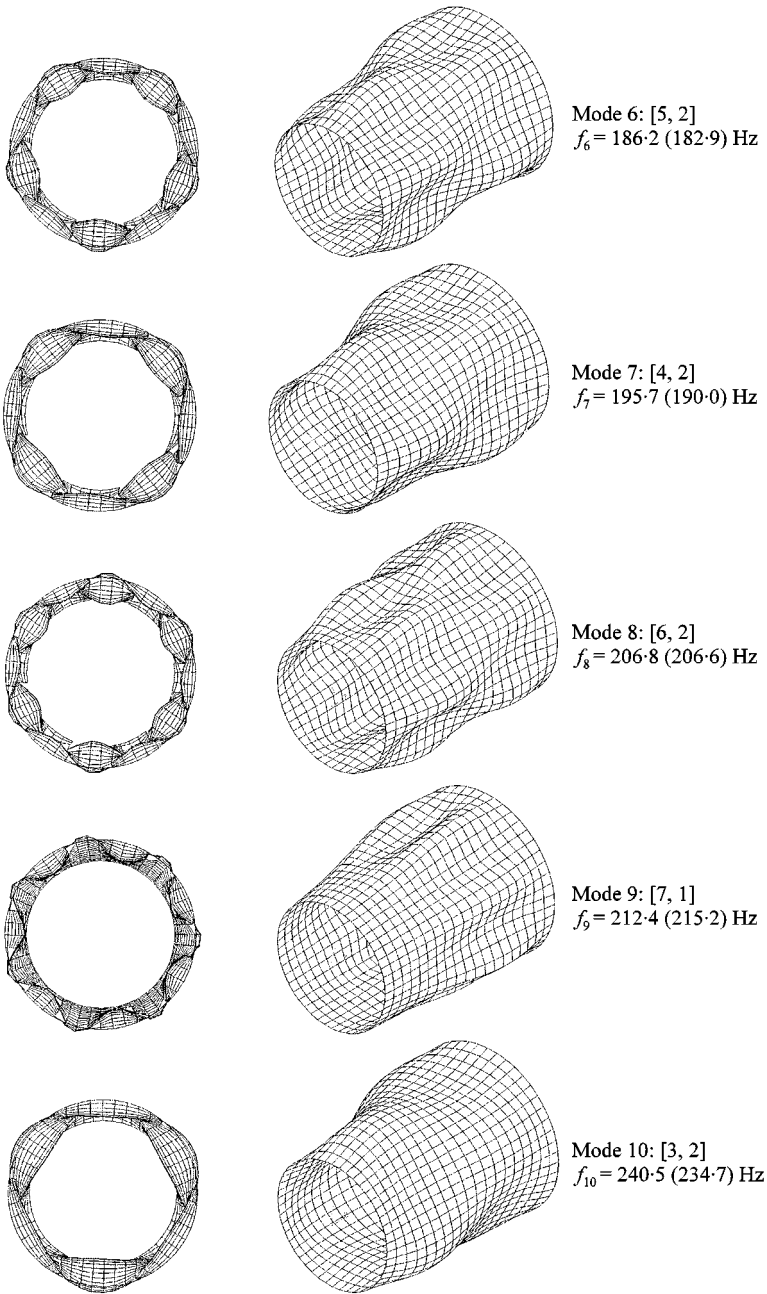


Figure 5. Continued.

circumferential supports, which is permissible for this particular boundary condition; for a *cylindrical* shell, this would amount to a zero-frequency rigid-body motion. However, for a conical panel, such a motion will cause the supports to induce a circumferential hoop strain in the shell, and hence involve elastic deformations and inertia effects, thus resulting in a non-zero frequency. Clearly, the greater

the coning angle, the more severe will be the induced circumferential hoop strain, and hence the higher the natural frequency of this particular motion. No mention of this effect has been made by previous authors.

3.3. FURTHER ANALYTICAL RESULTS

To complete the analytical study, the four panels used as the basis for the experimental work (see section 3.4) were also the subject of a full theoretical investigation. The panels are defined by the geometric and material data presented in Table 4, and then analyzed according to various sets of idealized classical boundary conditions. (The two sets of most interest here comprised simply supported or clamped circumferential ends in conjunction with free longitudinal edges.) Results for the first 10 natural frequencies of each panel are presented in Tables 5–8 (Figures 6 and 7 show a representative sample of the calculated natural modes for Test Panel # 1 subject to both circumferential ends being simply supported and clamped respectively). The h - p results have been calculated using a 10 element mesh with each element polynomially enriched to a level of $p = 8$ in order to guarantee a well-converged solution. Likewise, an additional set of (fully converged) results has also been computed using ANSYS. Good agreement between both sets of numerical results (to within 4%) can be seen for every combination of panel and boundary condition considered here.

TABLE 4

Geometric data relative to the Layer 2 mid-plane defining the four conical sandwich test panels used in this work

Test panel	R_0 (m)	R_T (m)	L (m)	h_1 (mm)	h_2 (mm)	h_3 (mm)	ϕ (deg)	α (deg)
1	0.228	0.560	0.728	0.50	12.44	0.50	90	24.5
2	0.228	0.560	0.728	0.50	12.44	0.50	120	24.5
3	0.401	0.497	0.995	0.50	12.44	0.50	90	5.5
4	0.427	0.528	0.995	0.50	23.91	0.50	90	5.8

Material data common to all four conical sandwich test panels used in this work

Face plate properties	T3 aluminium plate			
	$\rho = 2695 \text{ kg/m}^3$	$E = 72.40 \text{ GPa}$	$\nu = 0.33$	$G = 27.22 \text{ GPa}$
Core properties	5052/F40 aluminium flex-core			
	$\rho = 91.3 \text{ kg/m}^3$	$E_{xx} \approx 0 \text{ GPa}$	$\nu_{\theta x} = 0.0$	$G_{\theta z} = 0.159 \text{ GPa}$
		$E_{\theta\theta} \approx 0 \text{ GPa}$	$\nu_{x\theta} = 0.0$	$G_{zx} = 0.469 \text{ GPa}$
			$G_{x\theta} = 0 \text{ GPa}$	

TABLE 5

Comparison of theoretical results calculated for an open conical sandwich panel

Test panel no. 1			
Boundary condition	Frequency (Hz)	Current <i>h-p</i> method. Well converged $h = 10, p = 8$ 1808 d.o.f.	FEM Fully converged 8298 d.o.f.
	f_1	267.5	263.8
	f_2	339.6	335.6
	f_3	565.7	559.4
Around $x = 0$: C	f_4	596.4	598.0
Around $x = a$: C	f_5	655.7	658.0
Around $\theta = 0$: F	f_6	799.3	765.6
Around $\theta = \phi$: F	f_7	987.3	1014.8
	f_8	1006.5	1029.4
	f_9	1084.6	1083.1
	f_{10}	1204.6	1158.5
Boundary condition	Frequency (Hz)	Current <i>h-p</i> method. Well converged $h = 10, p = 8$ 2128 d.o.f.	FEM Fully converged 8568 d.o.f.
	f_1	219.8	219.6
	f_2	300.8	298.3
	f_3	494.4	498.0
Around $x = 0$: S	f_4	508.6	508.5
Around $x = a$: S	f_5	594.1	591.4
Around $\theta = 0$: F	f_6	752.5	719.8
Around $\theta = \phi$: F	f_7	847.2	869.9
	f_8	871.8	894.1
	f_9	1013.5	1008.1
	f_{10}	1141.1	1097.9

3.4. INITIAL EXPERIMENTAL WORK CONDUCTED ON OPEN CONICAL SANDWICH PANELS

An experimental programme was devised with the intention of furnishing some actual test data for each of the four conical sandwich panels described in Table 4 and thus complementing the theoretical study presented above. This was felt to be especially important in view of the limited amount of work that has been carried out in this specific subject area. However, once testing had commenced, it rapidly became apparent that there were some significant and unexpected differences between the experimental test samples and the theoretical models—hence no explicit results are quoted here.

These differences were subsequently identified as (a) constructionally-induced and (b) rig-induced, as explained in what follows.

TABLE 6

Comparison of theoretical results calculated for an open conical sandwich panel

Test panel no. 2			
Boundary condition	Frequency (Hz)	Current h - p method Well converged $h = 10, p = 8$ 1808 d.o.f.	FEM Fully converged 11 226 d.o.f.
	f_1	296.9	294.0
	f_2	303.7	299.3
	f_3	565.3	555.9
Around $x = 0$: C	f_4	609.5	612.8
Around $x = a$: C	f_5	655.3	652.2
Around $\theta = 0$: F	f_6	711.9	705.6
Around $\theta = \phi$: F	f_7	843.1	802.4
	f_8	974.1	979.9
	f_9	997.4	1027.5
	f_{10}	1051.8	1058.8
Boundary condition	Frequency (Hz)	Current h - p method Well converged $h = 10, p = 8$ 2128 d.o.f.	FEM Fully converged 11 592 d.o.f.
	f_1	254.7	253.7
	f_2	261.7	260.7
	f_3	490.8	487.7
Around $x = 0$: S	f_4	512.4	515.9
Around $x = a$: S	f_5	603.3	594.5
Around $\theta = 0$: F	f_6	687.1	683.5
Around $\theta = \phi$: F	f_7	794.3	755.6
	f_8	845.5	862.7
	f_9	861.6	883.7
	f_{10}	970.8	959.1

(a) Although the panels were constructed to the dimensions quoted in Table 4, it was observed that the skin-to-core bond likely accounted for a significant volume of adhesive which had not been included in the theoretical model. Also, there were core filler inserts used to prevent local crushing of the core when the support fixture bolts were tightened, and edge protection strips that had not been included in the mathematical models. Such constructional details were shown to increase the overall test panel mass above the theoretically predicted value by as much as 27%, see Table 9.

(b) Pairs of curved fibreglass angle brackets were used to support the test panels around their circumferential edges in an attempt to mimic the tail-boom sub-structure of a typical civil aircraft (see Figure 8). Although the fibreglass

TABLE 7

Comparison of theoretical results calculated for an open conical sandwich panel

Test panel no. 3			
Boundary condition	Frequency (Hz)	Current h - p method Well converged $h = 10, p = 8$ 1808 d.o.f.	FEM Fully converged 9054 d.o.f.
	f_1	199.6	195.4
	f_2	250.7	246.5
	f_3	447.1	441.0
Around $x = 0$: C	f_4	454.8	449.4
Around $x = a$: C	f_5	467.8	462.1
Around $\theta = 0$: F	f_6	628.6	598.6
Around $\theta = \phi$: F	f_7	732.7	734.5
	f_8	733.4	735.6
	f_9	865.6	836.7
	f_{10}	904.2	892.5
Boundary condition	Frequency (Hz)	Current h - p method Well converged $h = 10, p = 8$ 2128 d.o.f.	FEM Fully converged 9300 d.o.f.
	f_1	176.8	171.3
	f_2	232.7	226.1
	f_3	386.2	382.7
Around $x = 0$: S	f_4	413.5	393.6
Around $x = a$: S	f_5	448.5	442.7
Around $\theta = 0$: F	f_6	610.3	579.9
Around $\theta = \phi$: F	f_7	633.3	638.6
	f_8	673.7	641.9
	f_9	826.8	791.7
	f_{10}	862.5	855.6

bracket pairs fitted the contours of each test panel perfectly, and facilitated multiple bolting through the upper and lower flanges around both of their ends, the brackets nonetheless proved insufficiently stiff to represent a genuine clamped edge. This is a salutary example of the difference between an engineered item fabricated for "service" and its idealized representation in a theoretical model.

The net effect of the practical fabrication and mounting details described above was to reduce each set of test panel natural frequencies by anything between 12 and 20% of the corresponding theoretically obtained values. There seems little to be gained from presenting these data since one is not strictly comparing like with like.

TABLE 8

Comparison of theoretical results calculated for an open conical sandwich panel

Test panel no. 4			
Boundary condition	Frequency (Hz)	Current h - p method Well converged $h = 10, p = 8$ 1808 d.o.f.	FEM Fully converged 9882 d.o.f.
	f_1	252.7	250.7
	f_2	327.9	325.4
	f_3	496.6	490.2
Around $x = 0$: C	f_4	576.6	585.9
Around $x = a$: C	f_5	627.0	637.5
Around $\theta = 0$: F	f_6	888.3	839.0
Around $\theta = \phi$: F	f_7	922.5	921.7
	f_8	962.7	1009.4
	f_9	993.9	1043.3
	f_{10}	1048.5	1051.1
Boundary condition	Frequency (Hz)	Current h - p method Well converged $h = 10, p = 8$ 2128 d.o.f.	FEM Fully converged 10 140 d.o.f.
	f_1	194.7	195.1
	f_2	287.9	287.6
	f_3	461.3	453.3
Around $x = 0$: S	f_4	463.0	470.7
Around $x = a$: S	f_5	527.2	533.4
Around $\theta = 0$: F	f_6	805.5	806.3
Around $\theta = \phi$: F	f_7	840.0	843.4
	f_8	855.7	849.6
	f_9	869.1	882.8
	f_{10}	1046.6	1045.6

4. CONCLUSIONS

Open conical sandwich panels, consisting of a segment of a complete conical sandwich shell, figure occasionally as a stand-alone structural item, but are more commonly found as constituent components of larger, built-up structures such as the tapering tail section of a modern civil aircraft. A detailed formulation of an h - p sandwich panel finite element, based on a novel set of trigonometric assumed displacement functions, has been presented in this paper. The element so developed can be used to model both open conical sandwich panels or circumferentially closed conical sandwich frusta with equal facility. The convergence properties of this element have been established for different combinations of the h - and p -parameters, thereby assuring its integrity for more general use. Since very little work has

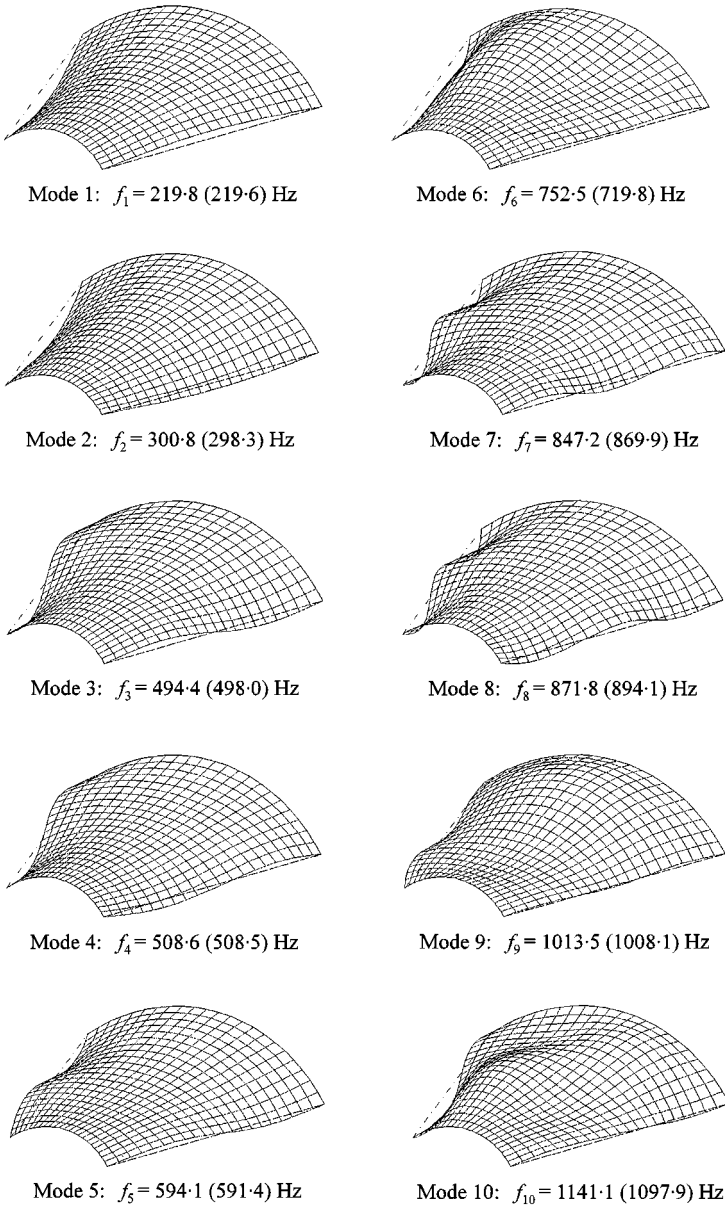


Figure 6. The first ten natural frequencies and modes of Test Panel no. 1 with its circumferential ends simply supported. (h - p results quoted with $h = 10$ and $p = 8$; ANSYS results in parentheses).

been reported on the vibration characteristics of either circumferentially-closed or open conical sandwich panels, the main thrust of this work has been to present and validate an efficient modelling technique, rather than to perform numerous parameter studies and sensitivity studies.

To this end, it has been shown that the level of mesh refinement which gives well-converged frequencies for one particular sandwich cone geometry almost certainly will not give similarly converged frequencies for a different geometry, so in

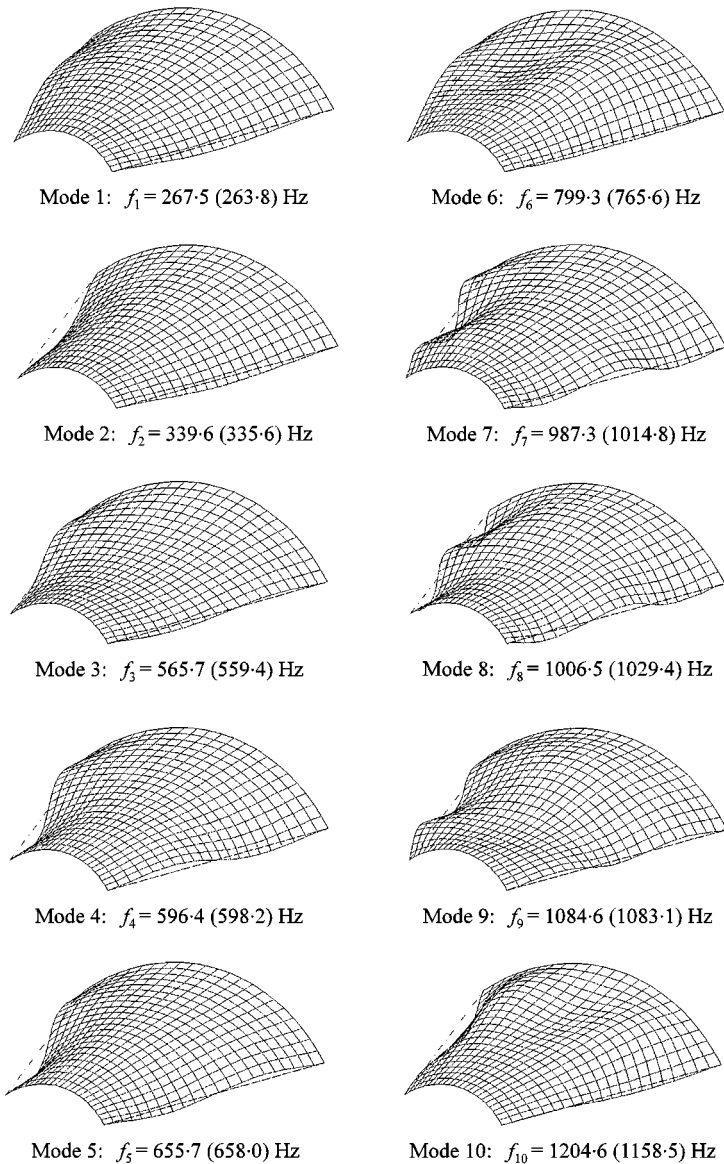


Figure 7. The first ten natural frequencies and modes of Test Panel no. 1 with its circumferential ends clamped. (h - p results quoted with $h = 10$ and $p = 8$; ANSYS results in parentheses).

general it will be necessary to validate the convergence of each and every case. This is especially important for conical sandwich panels, since their vibration behaviour is quite different from *cylindrical* sandwich panels, and it does not seem possible to predict what effect a certain parameter change will have on a conical panel, even if its effect on a similarly dimensioned cylindrical sandwich panel is already known.

One of the best ways to assess the relative computational merits of the h - p version of the FEM developed here and the h -version of the FEM that is commercially available is to compare the CPU time each requires to solve identical problems and

TABLE 9

Comparison of the measured and calculated masses of each test panel

Test panel no.	Measured mass (kg)	Calculated mass (kg)	% difference
1	2.42	1.90	27
2	3.19	2.53	26
3	3.25	2.70	20
4	4.60	3.66	26

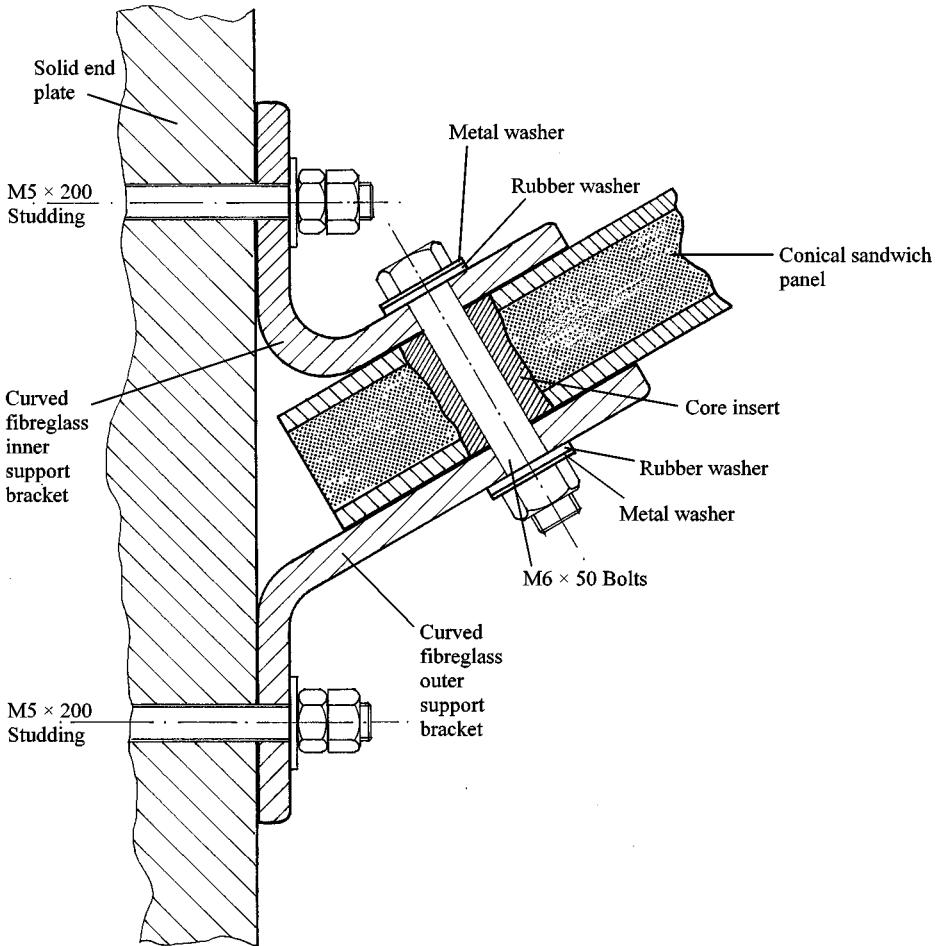


Figure 8. Details of the test-rig end fixtures, illustrating the means of providing a circumferential clamped edge support (longitudinal section).

furnish answers to similar accuracy. However, such a comparison is fraught with difficulties since both codes are written for completely different purposes and are hosted on different computer platforms. (The *h-p* code used here is essentially R&D

software written in FORTRAN 90, using various (non-vectorized) NAG subroutines—by contrast, ANSYS is a fully developed commercial code utilizing highly efficient wavefront solvers.) These disparate factors prevent any simple like-for-like comparisons. The next best performance measure, which is based on the total number of d.o.f. needed to define the resulting eigenproblem, is the one adopted here by the authors.

On this basis, the studies reported here have shown that the overall performance of the h - p formulation considerably exceeds that of the more general commercial software package. Perhaps this is not surprising when it is understood that the work presented here is tailored specifically to conical sandwich panels, whereas the commercial package makes use of a more general sandwich shell element. Even so, it is worth noting that by using the h - p version of the FEM in preference to the h -version, it is possible to obtain well-converged answers using only 25% of the latter's total number of degrees of freedom (see Tables 2, 3 and 5–8). The considerable savings in the final size of matrix-eigenvalue problem that result when compared with conventional finite element type analyses could usefully be employed should typical parameter studies, or repetitive calculations arising from an optimization algorithm, be required at the design stage.

It should also be noted that the methodology advanced here for a generic conical panel can also be used to analyze open or closed cylindrical sandwich shells ($\alpha = 0^\circ$, $R_0 = R_T$ set to the radius of the cylinder), and flat annular sectorial sandwich plates ($\alpha = 90^\circ$, R_0 set to the inner radius and R_T set to the outer radius of the plate).

Finally, two important points were highlighted by the practical work carried out here, namely the not insignificant mass of the core-to-face-plate adhesive and the mounting fixture insert fillers, and the finite flexibility of the panel mountings. If future, theoretical models are to be used to predict the vibration response of conical sandwich structures in a practical context, then it will be important that such models include (i) the inertial and elastic effects of the adhesive layers between the face plates and the core, and (ii) a more realistic representation of the boundary condition interface around the curved ends.

ACKNOWLEDGMENTS

The assistance rendered by the following organizations is gratefully acknowledged: EPSRC, under contract number GR/J 06306, for providing the financial support; and the Composites Workshop of British Airways Engineering, Heathrow Airport, for producing the test specimens.

REFERENCES

1. R. WANG 1992 *International SAMPE Symposium Exhibition*, **37**, 186–197. Sandwich construction in the “Starship”.
2. J. J. AZAR 1965 Ph.D. Thesis, University of Oklahoma. Axisymmetric free vibrations of sandwich shells of revolution.
3. C. W. BERT and J. D. RAY 1969 *International Journal of Mechanical Science* **11**, 767–778. Vibrations of orthotropic sandwich conical shells with free edges.

4. C. C. SUI and C. W. BERT 1970 *Journal of the Acoustical Society of America* **47**, 943–954. Free vibrational analysis of sandwich conical shells with free edges.
5. D. J. WILKINS, C. W. BERT and D. M. EGGLE 1970 *Journal of Sound and Vibration* **13**, 211–228. Free vibrations of orthotropic sandwich conical shells with various boundary conditions.
6. A. P. GUPTA and M. JAIN 1978 *Journal of Pure and Applied Mathematics* **9**, 1322–1336. Axisymmetric vibrations of conical sandwich shells.
7. P. V. NAVANEETHAKRISHNAN and N. RAVISRINIVAS 1993 *Second International Congress on Recent Developments in Air- and Structure-Borne Sound and Vibration*. Free asymmetric vibrations of layered conical shells by collocation with splines.
8. K. N. KHATRI 1992 *Proceedings of the Institution of Mechanical Engineers, Part C: Journal of Mechanical Engineering Science* **206**, 167–178. Vibration control of conical shells using viscoelastic materials.
9. L. WANG and R. XIA 1993 *Fuhe Cailiao Xuebao/Acta Materiae Compositae Sinica* **10**, 25–32. Effective approach for buckling, bending and vibration of anisotropic sandwiched composite conical shells.
10. T. C. RAMESH and N. GANESAN 1993 *Journal of Sound and Vibration* **166**, 531–538. Finite element based on a discrete layer theory for the free vibration analysis of conical shells.
11. T. C. RAMESH and N. GANESAN 1993 *Finite Elements in Analysis and Design* **13**, 17–29. Vibration and damping analysis of conical shells with constrained damping layer.
12. T. C. RAMESH and N. GANESAN 1994 *Journal of Sound and Vibration* **171**, 577–601. Finite element analysis of conical shells with a constrained viscoelastic layer.
13. K. N. KHATRI 1996 *Computers and Structures* **58**, 389–406. Axisymmetric vibration of multilayered conical shells with core layers of viscoelastic material.
14. K. N. KHATRI 1996 *Aeronautical Journal* **100**, 285–294. Asymmetric vibration of viscoelastically damped multilayered conical shells.
15. K. N. KHATRI 1996 *International Journal of Solids and Structures* **33**, 2331–2355. Antisymmetric vibration of multilayered conical shells with constrained viscoelastic layers.
16. K. N. KHATRI and N. T. ASNANI 1995 *Composite Structures* **33**, 143–157. Vibration and damping analysis of multilayered conical shells.
17. K. N. KHATRI and N. T. ASNANI 1996 *Journal of Sound and Vibration* **193**, 581–595. Vibration and damping of fiber reinforced composite material conical shells.
18. M. BARUCH 1996 *Composite Structures* **35**, 245. Comment on ‘Vibration and damping analysis of multilayered conical shells’.
19. A. K. NOOR, W. S. BURTON and C. W. BERT 1996 *Applied Mechanics Reviews* **49**, 155–199. Computational models for sandwich panels and shells.
20. K. M. LIEW, C. W. LIM and S. KITIPORNCHAI 1997 *Applied Mechanics Review* **50**, 431–444. Vibration of shallow shells: a review with bibliography.
21. K. H. HA 1990 *Computers and Structures* **37**, 397–403. Finite element analysis of sandwich plates: an overview.
22. O. C. ZIENKIEWICZ 1977 *The Finite Element Method*. New York: McGraw-Hill, Third edition.
23. O. C. ZIENKIEWICZ, J. P. DE S. R. GAGO and D. W. KELLY 1983. *Computers and Structures* **16**, 53–65. The hierarchical concept in finite element analysis.
24. A. PEANO 1976 *Computers and Mathematics with Applications* **2**, 211–224. Hierarchies of conforming finite elements for plane elasticity and plate bending.
25. B. GUO and I. BABUSKA 1986 *Computational Mechanics* **1**, 21–41. The h - p version of the finite element method, Part 1: the basic approximation results.
26. B. GUO and I. BABUSKA 1986 *Computational Mechanics* **1**, 203–220. The h - p version of the finite element method. Part 2. general results and applications.
27. L. DEMKOWICZ, J. T. ODEN, W. RACHOWICZ and O. HARDY 1989 *Computer Methods in Applied Mechanics and Engineering* **77**, 79–112. Toward a universal h - p adaptive finite element strategy, Part 1. Constrained approximation and data structure.

28. O. BESLIN and J. NICOLAS 1997 *Journal of Sound and Vibration* **202**, 633–655. A hierarchical functions set for predicting very high order plate bending modes with any boundary conditions.
29. C. W. LIM and K. M. LIEW 1995 *Engineering Structures* **17**, 63–70. Vibratory behaviour of shallow conical shells by a global Ritz formulation.
30. Technical Support Bulletin 120 (superceded), 15, 5052/F40 Aluminium Flex-Core. Hexcell Composites Ltd. Duxford, Cambridge CB2 4QD, U.K.
31. W. SOEDEL 1981 *Vibrations of Shells and Plates*. New York: Marcel Dekker Inc.
32. N. S. BARDELL, J. M. DUNSDON and R. S. LANGLEY 1997 *Composite Structures* **38**, 463–475. Free vibration analysis of coplanar sandwich panels.
33. NAG FORTRAN Library D01 AKF Mark 16, NAG Ltd, Wilkinson House, Jordan Hill Road, Oxford, U.K.
34. ANSYS Inc., 201 Johnson Road, Houston, PA 15342–1300, U.S.A.